On Reconstruction of the Dynamic Tortuosity Functions of Poroelastic Materials

M. Yvonne Ou

Department of Mathematical Sciences
University of Delaware
Newark, DE 19716, USA
mou@udel.edu

SYMPOSIUM ON THE ACOUSTICS OF PORO-ELASTIC MATERIALS, Dec. 16, 2014, KTH

Sponsored by NSF-DMS-0920852 (Math. Bio.) and NSF-DMS-1413039 (Inverse Problems)

Poroelastic Material

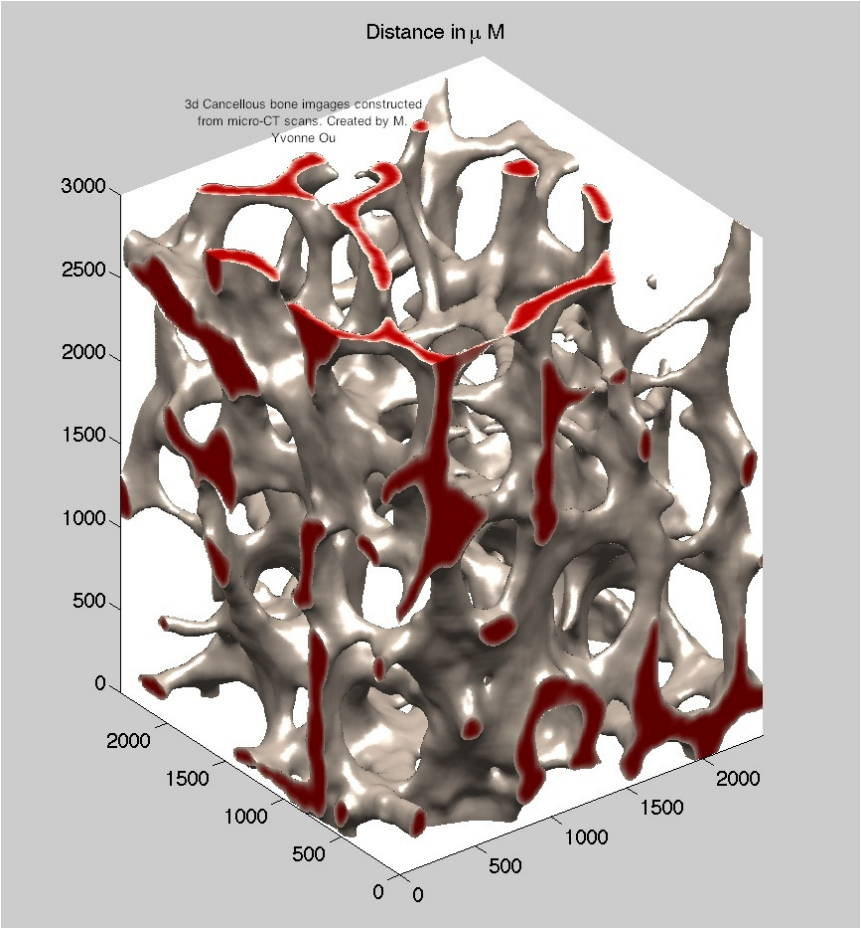

Figure: 3-D trabeculae reconstructed from micro-CT scans provided by L. Cardoso. [MYO-2011]. Elastic frame with viscous pore fluid

Outline

- Wave propagation in poroelastic composites and frequency-dependent mass coupling and dissipation (drag force).
- Stieltjes functions and the Integral Representation formula (IRF) for dynamic permeability with measure $d\lambda$
- Reconstruction of dynamic permeability from finite data sets
- IRF for dynamic tortuosity with measure $d\sigma$.
- Relations between the microstructure and tortuosity in terms of the moments of measure $d\sigma$

Biot's equations for waves in poroelastic materials

M. A. Biot, *Theory of propagation of elastic waves in a fluid-saturated porous solid*, J. Acoustical Society of America (JASA) (1956a (5510), 1956b (2412)).

Web of Science: `We are sorry...The citation map you are trying to create contains more papers (nodes) than we can process.`

Three pieces of physics

- Strain-stress relation
- Kinetic energy
- Energy dissipation

$\boldsymbol{u}$: displacement vector for solid

$\boldsymbol{U}$: displacement vector for fluid

* Stress tensor acting on the solid part: τ_{ij}, $i, j = 1, 2, 3$
* Stress tensor acting on the fluid part: $s\delta_{ij}$, $s = -\beta p$, β: porosity.
* Strain tensor in the solid: $e_{ij} = \frac{1}{2}(\frac{\partial u_i}{\partial x_j} + \frac{\partial u_j}{\partial x_i})$, $i, j = 1, 2, 3$
* Strain tensor in the fluid: $\epsilon = \nabla \cdot \boldsymbol{U}$

Coupled stress-strain relation $\tau_{ij} = 2N e_{ij} + \delta_{ij}(Ae + Q\epsilon)$

2nd-order formulation, low-frequency regime, isotropic case

Biot's Dynamic equations, 1956-a

$$N\nabla^2 \boldsymbol{u} + \nabla[(A+N)e + Q\epsilon] = \frac{\partial^2}{\partial t^2}(\rho_{11}\boldsymbol{u} + \rho_{12}\boldsymbol{U}) + \mathrm{b}\,\frac{\partial}{\partial t}(\boldsymbol{u} - \boldsymbol{U})$$

$$\nabla[Qe + R\epsilon] = \frac{\partial^2}{\partial t^2}(\rho_{12}\boldsymbol{u} + \rho_{22}\boldsymbol{U}) - \mathrm{b}\,\frac{\partial}{\partial t}(\boldsymbol{u} - \boldsymbol{U})$$

Dissipation coeff. $b := \frac{\beta^2\eta}{\kappa}$ is constant $\Longleftrightarrow$ laminar flow in pore space

β: porosity, η: dynamic viscosity

κ: static permeability

First order formulation, low-freq.

$\boldsymbol{v} := \dot{\boldsymbol{u}}, \quad \boldsymbol{q} := \beta(\dot{\boldsymbol{U}} - \dot{\boldsymbol{u}}), \quad p := -\frac{Qe+R\epsilon}{\beta}$ (pore pressure)

- Stress-strain relations

$$\begin{aligned}
\partial_t \tau_{xx} &= c_{11}^u \partial_x v_x + c_{13}^u \partial_z v_z + \alpha_1 M(\partial_x q_x + \partial_z q_z) \\
\partial_t \tau_{zz} &= c_{13}^u \partial_x v_x + c_{33}^u \partial_z v_z + \alpha_3 M(\partial_x q_x + \partial_z q_z) \\
\partial_t \tau_{xz} &= c_{55}^u (\partial_z v_x + \partial_x v_z) \\
\partial_t p &= -\alpha_1 M \partial_x v_x - \alpha_3 M \partial_z v_z - M(\partial_x q_x + \partial_z q_z)
\end{aligned}$$

- Equations of motion

$$\rho \partial_t v_i + \rho_f \partial_t q_i = [\nabla \cdot \tau]_i$$

(Darcy's law in x_i direction) $\quad \rho_f \partial_t v_i + m_i \partial_t q_i + \left(\frac{\eta}{\kappa_i}\right) q_i = -\partial_{x_i} p$

$m_i := \frac{\rho_f \alpha_{\infty i}}{\beta}$, $\alpha_{\infty i}$: inf-freq tortuosity in the i-th direction (difficult to measure)

Low-freq. Biot equations and ultrasound in cancellous bones

Problem: low-frequency Biot equations underestimate wave dissipation when compared with experiment.

Solution: High-frequency correction is made in frequency domain.

Fourier transform to frequency domain

$$\tilde{f}(\omega) := \frac{1}{\sqrt{2\pi}} \int_0^\infty v(t) e^{i\omega t}\, dt$$

Three approaches to high-freq. corrections

- Biot's correction to $\tilde{b}$: too restrictive in terms of pore geometry
- JKD correction introducing dynamic tortuosity and permeability function: a tunable parameter for geometry thus more flexible. However, the two JKD functions are the **simplest** form of the functions that satisfy the necessary causality properties. **There is no reason all pore geometries correspond to these specific function forms.**
- Torquato-Avellaneda's integral representation formula (IRF) for the dynamic permeability function: valid for all pore geometries **The most general correction.**

For the first order formulation, high-freq. correction is made to the dynamic tortuosity function.

Tortuosity and permeability, M. Matyka and Z. Koza, 2012

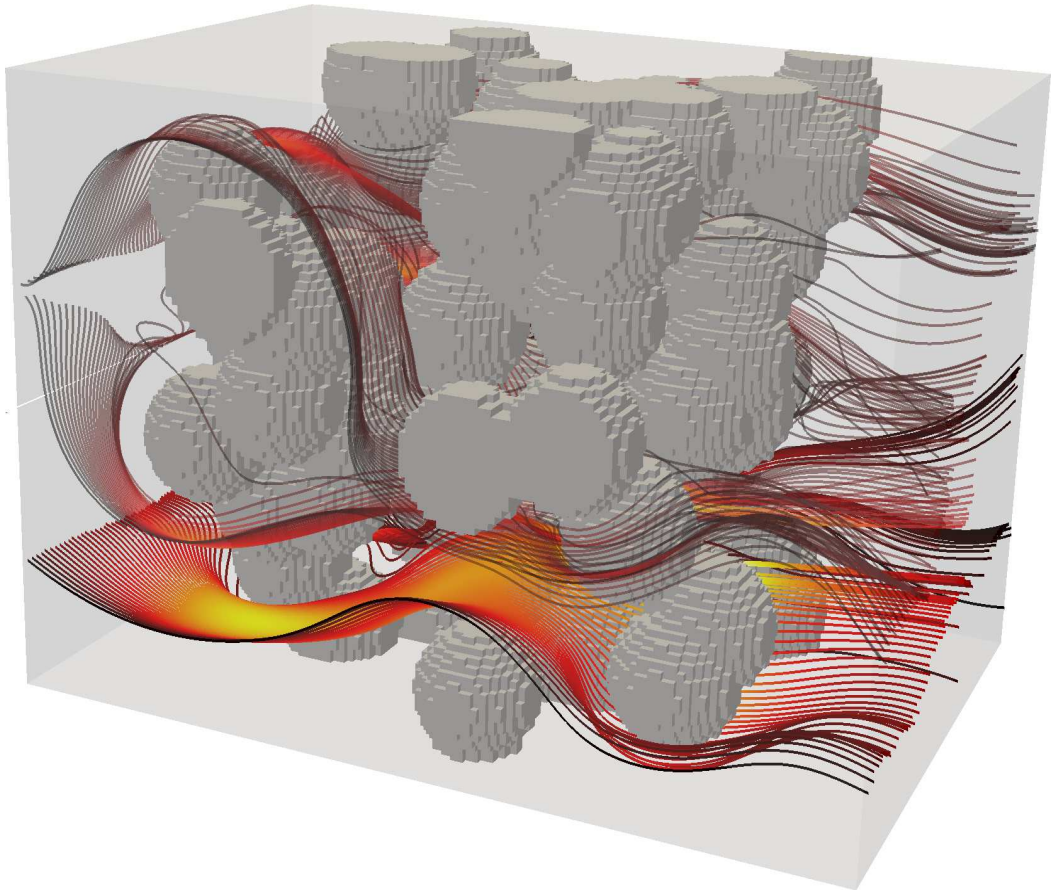

FIGURE 1. Streamlines in the fluid flow through three-dimensional random model of porous media at porosity $\varphi = 0.6$ and tortuosity T=1.15.

Dynamic permeability and tortuosity

Dynamic permeability function $K(\omega)$

$$-i\omega\beta(\widetilde{\boldsymbol{U}} - \widetilde{\boldsymbol{u}}) = \frac{K(\omega)}{\eta}(-\nabla\widetilde{p} + \rho_f\omega^2\widetilde{\boldsymbol{u}}) \tag{1}$$

Dynamic tortuosity function $\alpha(\omega)$

$$\alpha(\omega)\rho_f(-i\omega)^2(\widetilde{\boldsymbol{U}} - \widetilde{\boldsymbol{u}}) = (-\nabla\widetilde{p} + \rho_f\omega^2\widetilde{\boldsymbol{u}}), \tag{2}$$

Example: (low-freq. Darcy's law)

$$\rho_f\partial_t v_x + \left(\frac{\rho_f\alpha_{\infty 1}}{\beta}\right)\partial_t q_x + \left(\frac{\eta}{\kappa_1}\right)q_x = -\partial_x p \Longleftrightarrow \alpha_1(\omega) = \alpha_{\infty 1} + \frac{\eta\beta/(\kappa_1\rho_f)}{-i\omega}$$

Time-domain High-freq. Darcy's law has a memory term

$$(2) \text{ and } (1) \Rightarrow \alpha(\omega) = \frac{i\eta\beta}{\omega\rho_f}K^{-1}(\omega) \text{ for } \omega \neq 0$$

Note: $K(0) = \kappa = K_0$ =static permeability

JKD Model

In [Johnson-Koplik-Dashen-1987], 1077, by extending $\alpha(\omega)$ and $K(\omega)$ to complex ω-plane and using causality argument, the simplest forms are derived

$$\alpha_D(\omega) = \alpha_\infty \left(1 - \frac{\eta\phi}{i\omega\alpha_\infty\rho_f K_0}\sqrt{1 - i\frac{4\alpha_\infty^2 K_0^2\rho_f\omega}{\eta\Lambda^2\phi^2}}\right)$$

$$K_D(\omega) = K_0 / \left(\sqrt{1 - \frac{4i\alpha_\infty^2 K_0^2\rho_f\omega}{\eta\Lambda^2\phi^2}} - \frac{i\alpha_\infty K_0\rho_f\omega}{\eta\phi}\right).$$

with the tunable geometry-dependent constant Λ, $\phi = \beta$ (porosity).

inf-freq. model as $\omega \to \infty$

$$\alpha(\omega) \to \alpha_\infty\left(1 + \sqrt{\frac{i\eta}{\rho_f\omega}}\frac{2}{\Lambda}\right),\ K(\omega) \to \frac{i\eta\phi}{\alpha_\infty\rho_f\omega}\left(1 - \sqrt{\frac{i\eta}{\rho_f\omega}}\frac{2}{\Lambda}\right)$$

Models for ultrasound in cancellous bone

Hosakawa 2006, *Ultrasonics*

Table 3
Biot's parameters of bovine cancellous bone models with parallel and perpendicular trabecular orientations

	Parallel	Perpendicular
Young's modulus of solid bone E_s	22.0 GPa	22.0 GPa
Poisson's ratio of solid bone v_s	0.32	0.23
Bulk modulus of bone marrow K_f	2.0 GPa	2.0 GPa
Density of solid bone ρ_s	1960 kg/m^3	1960 kg/m^3
Density of bone marrow ρ_f	930 kg/m^3	930 kg/m^3
Poisson's ratio of trabecular frame v_b	0.32	0.23
Variable r	0.25	0.25
Viscosity of bone marrow η	1.5 P s	1.5 P s
Parameter n	1.46	2.14
Pore size a_0	1.35 mm	1.35 mm
Permeability k	3×10^{-8}	3×10^{-9}
Porosity β	0.83	0.83
Resistance coefficients γ_{ii} $(i = x, y)$	1.0×10^6	1.0×10^6
Resistance coefficient γ_{xy}	1.0×10^7	1.0×10^7

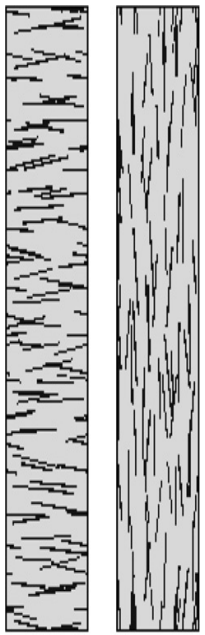

Fig. 2. Geometric drawings of bovine cancellous bone models in the viscoelastic FDTD method, with (a) parallel and (b) perpendicular trabecular orientations.

Fellah et. al. 2004, 2006, *JASA*: inf-freq. model.

Biot's model parameters of cancellous bone	M1	M2	M3
Thickness L (cm)	0.7	0.5	0.38
Density ρ_s (kg/m^3)	1960	1960	1960
Porosity ϕ	0.83	0.77	0.88
Tortuosity α_∞	1.05	1.01	1.02
Viscous characteristic length Λ (μm)	5	2.7	5
Bulk modulus of the elastic solid Ks (GPa)	20	20	26
Bulk modulus of bone skeletal frame Kb (GPa)	3.3	4	1.3
Shear modulus of the frame N (GPa)	2.6	1.7	0.35

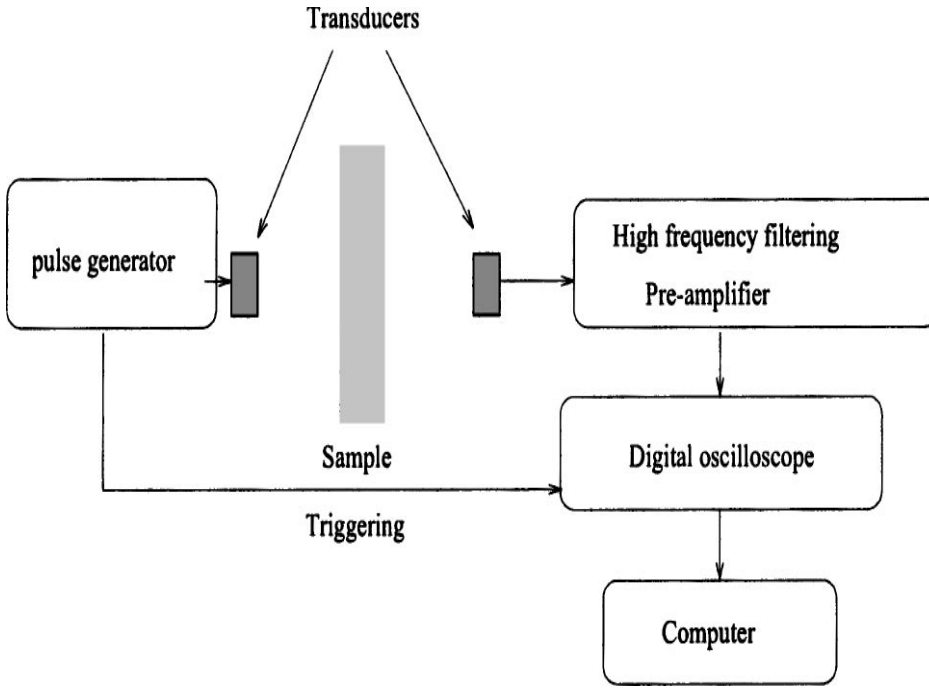

FIG. 15. Experimental setup for ultrasonic measurements.

In Fellah 2006, ϕ, α_∞, Λ, K_b and N are sought after by solving the inverse problem.

Questions....

- How does the microstructural information of pore space quantitatively enter the permeability?
- Must all permeabilities have the simplest form as suggested in the JKD model? **No.**
- Given a set of permeability data at various frequencies, how well can we interpolate/extrapolate?
- How to numerically handle the memory terms in a time domain solver?

The key is in the mathematical structure of $K(\omega)$

Integral representation formula for $K(\omega)$

[Avellaneda-Torquato-91, 133]

For any pore geometry,

$$\frac{F}{\nu} K(\omega) = \int_0^{\Theta_1} \frac{\Theta \, dG(\Theta)}{1 - i\omega\Theta}, \text{ with } G(\Theta) = \frac{\sum_{\Theta_n \le \Theta} b_n^2}{\sum_{n=1}^{\infty} b_n^2}$$

Note: dG is a probability measure (positive measure), which contains all geometric information of the pore space. $F = \frac{\alpha_\infty}{\phi}$, ν: kinetic viscosity. b_n depends on the spectrum of the Stokes equation in pore space and the initial applied flow direction e.

$$\triangle \Psi_n + \nabla Q_n = -\epsilon_n \Psi_n \text{ and } \nabla \cdot \Psi_n = 0 \text{ in } \mathcal{V}_1, \ \Psi_n = 0 \text{ on } \partial\mathcal{V}_1,$$

$0 < \epsilon_1 \le \epsilon_2 \le \cdots$ and $\epsilon_n \to \infty$ as $n \to \infty$. $\Theta_n := (\nu\epsilon_n)^{-1}$ are the viscous relaxation times and Θ_1 referred to as the principal viscous relaxation time. The eigenfunctions are orthonormal in the sense

$$\frac{1}{|\mathcal{V}_1|} \int_{\mathcal{V}_1} \Psi_m(\boldsymbol{x}) \cdot \Psi_n(\boldsymbol{x}) \, d\boldsymbol{x} = \delta_{mn} \text{ (Kronecker delta)}, \ b_n = \frac{1}{|\mathcal{V}_1|} \int_{\mathcal{V}_1} \boldsymbol{e} \cdot \Psi_n(\boldsymbol{x}) \, d\boldsymbol{x} \tag{3}$$

New Variables

ω	$s := -i\omega$	$\xi := -\frac{1}{s}$
$K(\omega)$	$P(s) := \left(\frac{F}{\nu}\right) K(is)$	$R(\xi) := -sP(s)$

$$P(s) := \left(\frac{F}{\nu}\right) K(is) = \int_0^{\Theta_1} \frac{\Theta\, dG(\Theta)}{1+s\Theta} =: \int_0^{\Theta_1} \frac{d\lambda(\Theta)}{1+s\Theta}$$

$$R(\xi) := -s\left(\frac{F}{\nu}\right) K(is) = -sP(s) = \int_0^{\Theta_1} \frac{\Theta\, dG(\Theta)}{\xi - \Theta}$$

Note: JKD model satisfies this IRF as well (can be shown using Herglotz function theory [MYO-2014])

Stieltjes function

Definition (Stieltjes function)

A Stieltjes function $f(z)$ for z on the extended complex plane has the following form

$$f(z) = \int_a^b \frac{d\mu(t)}{z - t} \tag{4}$$

where a, b are extended real numbers and $\mu(t)$ is a bounded, non-decreasing real function.

$$R(\xi) := -s\left(\frac{F}{\nu}\right) K(is) = -sP(s) = \int_0^{\Theta_1} \frac{\Theta\, dG(\Theta)}{\xi - \Theta}$$

is a Stieltjes function. Note: $\xi = -\frac{i}{\omega}$.

Multipoint Padé approximates of Stieltjes functions

Theorem ([Gelfgren-1978])

Let f be a Stieltjes function. Let $P_{n-1}(z)$ and $Q_n(z)$ be polynomials of degree at most $n-1$ and n, respectively, satisfying the relations ($k_1+k_2+k_3=2n$)

$$\begin{cases} f(z)Q_n(z) - P_{n-1}(z) = A(z)\prod_{j=1}^{k_1}(z-x_j)\prod_{j=1}^{k_2}(z-z_j)(z-\overline{z}_j) \\ f(z)Q_n(z) - P_{n-1}(z) = B(z)z^{n-k_3-1} \end{cases}$$

where $A(z)$, $B(z)$ are analytic in $\mathbb{C}\setminus[a,b]$, $B(z)$ bounded at ∞, $x_1,\cdots,x_{k_1}\in\mathbb{R}\setminus[a,b]$, $z_1,\cdots,z_{k_2}\in\mathbb{C}\setminus\mathbb{R}$. Then $[n-1/n]_f(z) := \frac{P_{n-1}(z)}{Q_n(z)} = \int_a^b \frac{d\beta(t)}{z-t}$ for some bounded, non-decreasing function $\beta(t)$.

$[n-1/n]_f(z) = \sum_{k=1}^{n} \frac{r_k}{z-p_k}$, with $r_k>0$ and $p_k\in(a,b)$ for $k=1,\cdots,n$.

Reconstruction from finite data set $K(\omega_j)$

Given $R(\xi_j)$, $j = 1, \cdots, M$, to construct $[M-1/M]_R(\xi)$. Data at conjugate points can be obtained through symmetry

$$R(\overline{\xi_j}) = \int_0^{\Theta_1} \frac{d\lambda(\theta)}{\overline{\xi_j} - \theta} = \overline{\int_0^{\Theta_1} \frac{d\lambda(\theta)}{\xi_j - \theta}} = \overline{R(\xi_j)}$$

$$[M-1/M]_R(\xi) = \sum_{j=1}^{M} \frac{r_j}{\xi - p_j},\ r_j > 0, 0 < p_j < \Theta_1$$

$$K(\omega) \approx \frac{\nu}{F} \sum_{j=1}^{M} \frac{r_j}{1 - i\omega p_j},\ \mathcal{F}^{-1}[K](t) \approx \left(\frac{\nu}{F}\right) \sum_{j=1}^{M} \left(\frac{r_j}{p_j}\right) e^{-\frac{t}{p_j}}$$

Moments: $$\mu_j(d\lambda) := \int_a^b \theta^j \, d\lambda(\theta) \approx \sum_k p_k^j r_j$$

Note: $\mu_0(d\lambda) = \frac{FK_0}{\nu} = \frac{\alpha_\infty K_0}{\nu\phi} \Rightarrow \alpha_\infty$ can be computed from permeability data

IRF for Dynamic Tortuosity

Theorem (MYO-2014)

The dynamic tortuosity $\alpha(\omega) = \frac{i\eta\phi}{\omega\rho_f} K^{-1}$ *has the following integral representation formula for* ω *such that* $-\frac{i}{\omega} \in \mathbb{C} \setminus [0, \Theta_1]$

$$\alpha(\omega) = a\left(\frac{i}{\omega}\right) + \int_0^{\Theta_1} \frac{d\sigma(\Theta)}{1 - i\omega\Theta}$$

for some positive measure $d\sigma$, *with* $a = \frac{\eta\phi}{\rho_f K_0}$. $\mu_0(d\sigma) = \frac{\alpha_\infty}{\mu_0^2(d\lambda)}\mu_1(d\lambda)$

(1) $\alpha(\omega) \to \alpha_\infty$ as $\omega \to \infty$, $d\sigma$ has a Dirac mass at $\Theta = 0$ with strength α_∞.
(2) $h(\xi) := a - \frac{\alpha_\infty}{\xi R(\xi)} = a + i\omega\alpha(\omega)$ is a Stieltjes function and $h(\bar{\xi}) = \overline{h(\xi)}$
(3) $\alpha(\omega) \approx \frac{a}{-i\omega} + \sum_{j=1}^{M} \frac{r_j}{-i\omega - p_j}$, $r_j > 0$, $p_j \in (-\infty, -\frac{1}{\Theta_1})$
(4) $\mathcal{F}^{-1}[\alpha](t) = a\delta(t) + \sum_{j=1}^{M} r_j e^{p_j t}$ Provides an efficient way to handle the memory term and settles a debate in poroelasticity

Moments and effective properties [MYO-2014]

$$\mu_0(d\lambda) = \frac{\alpha_\infty K_0}{\phi\nu}$$

$$\alpha_\infty = \frac{\mu_0(d\sigma)\mu_0^2(d\lambda)}{\mu_1(d\lambda)}$$

Specializing the result to JKD model, the microstructure-dependent parameter Λ (a weighted average of volume-to-surface ratio of the dynamically connected pore space) satisfies

$$\Lambda = \sqrt{\frac{2K_0\alpha_\infty^2}{\phi[\mu_0(d\sigma^D) - \alpha_\infty]}} = \sqrt{\frac{2K_0\alpha_\infty}{\phi[\frac{\mu_1(d\lambda^D)}{\mu_0^2(d\lambda^D)} - 1]}}$$

Note: Empirical formula in literature $\Lambda \approx \sqrt{\frac{2\alpha_\infty K_0}{\phi/4}}$!

Formulation for Reconstruction

$P(s_j) = \int_0^{\Theta_1} \frac{\Theta dG(\Theta)}{1+s_j\Theta} \approx [M-1/M]_P(s) := \frac{a_0+a_1 s_j+\cdots+a_{M-1}s_j^{M-1}}{1+b_1 s_j+\cdots+b_M s_j^M}$, $j = 1 \sim 2M$ Given the data $(s_j, P(s_j))$, $s_j \neq 0$, $j = 1, \cdots, M$, let $s_{j+M} = -s_j$, $P(s_{j+M}) = \overline{P(s_j)}$ and $P_m := P(s_m)$, $m = 1, \cdots, 2M$. Solve $A\boldsymbol{x} = \boldsymbol{d}$

$$A = \begin{pmatrix} 1 & s_1 & s_1^2 & \cdots & s_1^{M-1} & -P_1 s_1 & -P_1 s_1^2 & -P_1 s_1^3 & \cdots & -P_1 s_1^M \\ 1 & s_2 & s_2^2 & \cdots & s_2^{M-1} & -P_2 s_2 & -P_2 s_2^2 & -P_2 s_2^3 & \cdots & -P_2 s_2^M \\ \vdots & \vdots & \vdots & \vdots & \vdots & \vdots & \vdots & \vdots & \vdots & \vdots \\ 1 & s_{2M} & s_{2M}^2 & \cdots & s_{2M}^{M-1} & -P_{2M} s_{2M} & -P_{2M} s_{2M}^2 & -P_{2M} s_{2M}^3 & \cdots & -P_{2M} s_{2M}^M \end{pmatrix}$$

$= A_r + i\, A_i := Real(A) + i\, Imag(A)$

$$\begin{aligned} \boldsymbol{x} &= (a_0, a_1, \cdots, a_{M-1}, b_1, b_2, \cdots, b_M) \\ \boldsymbol{d} &= (P_1 \ P_2 \ \cdots \ P_{2M})^t \end{aligned}$$

$$[M-1/M]_P(s) := \frac{a_0 + a_1 s + \cdots + a_{M-1} s^{M-1}}{1 + b_1 s + \cdots + b_M s^M} = \sum_{j=1}^{M} \frac{r_j}{s - p_j} \Rightarrow \boldsymbol{x} \in \mathbb{R}^{2M}$$

Algorithm [MYO-2014]

1. Rescale each column $\boldsymbol{a}_j$, $j = 1, \cdots, 2M$ of A by $C := diag\{\|\boldsymbol{a}_j\|_2^{-1}\}_{j=1}^{2M}$. Let
$$A\boldsymbol{x} = (AC)(C^{-1}\boldsymbol{x}) =: B\boldsymbol{y}$$
2. Let
$$\hat{B} := \begin{pmatrix} B_r \\ B_i \end{pmatrix}, \ \hat{\boldsymbol{d}} := \begin{pmatrix} \boldsymbol{d}_r \\ \boldsymbol{d}_i \end{pmatrix}.$$
Solve the overdetermined system $\hat{B}\boldsymbol{y} = \hat{d}$ in least square sense with Tikhonov regularization
$$\min_{\boldsymbol{y}} \|\hat{B}\boldsymbol{y} - \hat{\boldsymbol{d}}\|_2^2 + \gamma^2\|\boldsymbol{y}\|_2^2$$
L-curve method is used for choosing the regularization parameter γ
3. Rescale $\boldsymbol{x} = C\boldsymbol{y}$.
4. Apply partial fraction decomposition to the resulting $2M$ Padé approximant. Retain the poles in $(-\infty, -\frac{1}{C_1}] \cup \{-\frac{1}{\xi_p}\}$ with positive weights.

JKD permeability moments from data $K(\omega_j)$ [MYO-2014]

Figure: Relative error of $\mu_1(d\lambda^D), \cdots, \mu_9(d\lambda^D)$ approximated from M data points in $[1, 51]$Hz

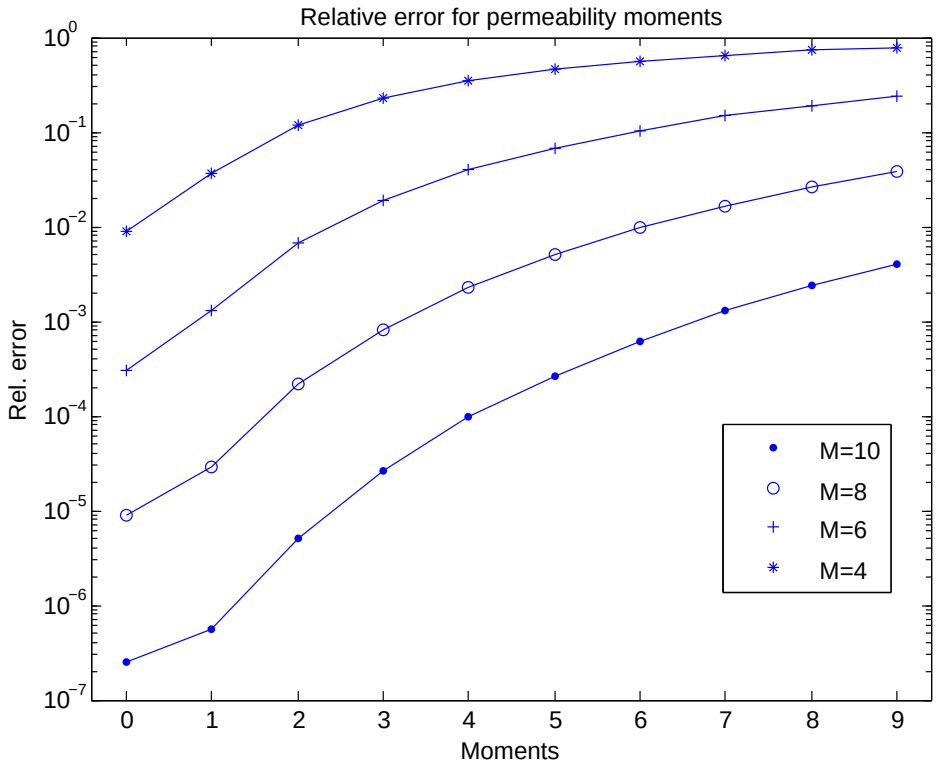

Reconstructed JKD Tortuosity from data $K(\omega_j)$ [MYO-2014]

Figure: . Max. Rel. Error for $\omega \in [1, 51]$ Hz and $\omega \in [0.75, 4]$ MHz. Linear convergence!

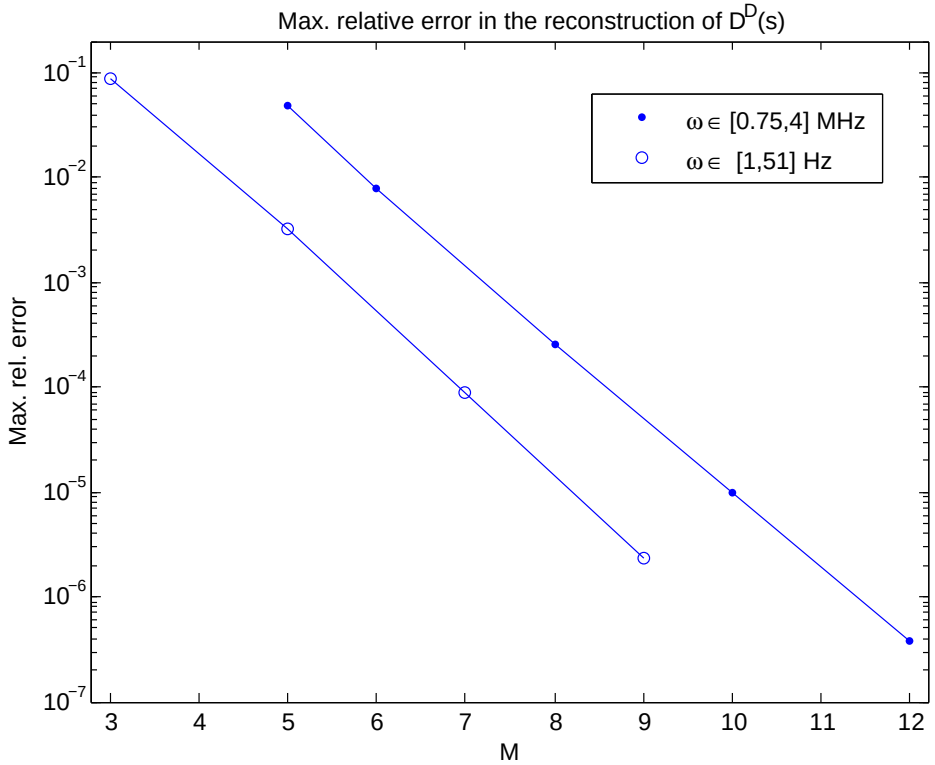

On reconstruction of dynamic permeability and tortuosity from data at distinct frequencies, Inverse Problems 30(9) 095002, 2014